

# Thin-film channel waveguide electro-optic modulator in epitaxial BaTiO<sub>3</sub>

D. M. Gill,<sup>a)</sup> C. W. Conrad,<sup>a)</sup> G. Ford,<sup>b)</sup> B. W. Wessels,<sup>a,b)</sup> and S. T. Ho<sup>a)</sup>  
*Materials Research Center, Northwestern University, Evanston, Illinois 60208*

(Received 28 February 1997; accepted for publication 23 July 1997)

We report on a thin-film channel waveguide electro-optic modulator fabricated in epitaxial BaTiO<sub>3</sub> on MgO. Films had an effective dc electro-optic coefficient of  $r_{\text{eff}} \sim 50 \pm 5$  pm/V and  $r_{\text{eff}} \sim 18 \pm 2$  pm/V at 5 MHz for  $\lambda \sim 1.55$   $\mu\text{m}$  light. Extinction ratios of 14 dB were obtained. The electro-optic effect decreases to  $\sim 60\%$  of the dc value at 1 Hz, 50% of the dc value at 20 kHz, and  $\sim 37\%$  of the dc value at 5 MHz. © 1997 American Institute of Physics. [S0003-6951(97)00539-1]

Thin-film ferroelectrics offer unique physical characteristics that could dramatically improve the performance of many integrated optic devices. Potential applications include low-voltage electro-optic switching,<sup>1</sup> compact low-threshold gain devices,<sup>2</sup> and second-harmonic generation.<sup>3</sup> The realization of active thin-film devices has been hindered by difficulty in fabricating low-loss films and channel waveguides. Recent advances in epitaxial deposition of oxides have now made it possible to synthesize layers of sufficient optical quality to form low-loss waveguides.<sup>4</sup> We have recently demonstrated highly confining ( $\Delta n \sim 0.6$ ), relatively low-loss thin-film channel waveguides in epitaxially grown BaTiO<sub>3</sub> on MgO.<sup>5</sup> BaTiO<sub>3</sub> is an attractive candidate for thin-film integrated optics due to its large electro-optic coefficients.<sup>6</sup> In this letter, we report on thin-film, BaTiO<sub>3</sub> channel waveguide structures with the potential for traveling-wave electro-optic modulator applications.

Films were synthesized by low-pressure metalorganic chemical vapor deposition.<sup>7</sup> The metalorganic precursors employed were titanium tetra-isopropoxide and barium hexafluoroacetylacetonate tetraglyme. Argon was used as the carrier gas, and O<sub>2</sub> bubbled through deionized water was used as the reactant gas. The introduction of water vapor was necessary for removal of the fluorine in the form of HF present in the fluorinated barium precursor. The films were deposited on (001) oriented MgO crystals at 725 °C at a growth rate of approximately 100 nm/h. Atomic force microscopy was used to analyze the surface morphology of the films.

X-ray diffraction indicated that the films were phase pure BaTiO<sub>3</sub>. Diffractometer measurements indicated single, broad ( $h00$ ) peaks with no tetragonal splitting.<sup>8</sup> The measured in-plane lattice parameter is 4.011 Å. Epitaxial alignment of the film to the substrate was confirmed with phi scans of the off-axis {220} planes in the BaTiO<sub>3</sub> crystal lattice, and the requisite fourfold symmetry was observed.

Waveguides were fabricated in a  $\sim 0.32$   $\mu\text{m}$  thick BaTiO<sub>3</sub> film. The film had a root-mean-square (rms) surface roughness of 13 nm and was subsequently mechanically planarized to a  $\sim 5$  nm rms surface roughness. Planarizing the film before photolithographic patterning greatly improves the quality of the waveguides produced, most likely due to an improved adhesion between the photoresist and the film sur-

face. Planarization also significantly reduces the surface scattering losses.<sup>9</sup> The propagation loss in a  $\sim 300$  nm thick planarized waveguide is, typically,  $\sim 5$  dB/cm for 1.5  $\mu\text{m}$  light. Waveguide ridges were defined by wet etching the films in a 1% HF water solution for 90 s. Waveguide ridge heights were measured to be 40 nm using an Alpha step profilometer. Coplanar electrodes were prepared using conventional lift-off techniques with 150 nm thick thermally evaporated Al. Figure 1 shows a schematic of the device.

The electro-optic response of the waveguide structure was measured by end firing either 1.3 or 1.5  $\mu\text{m}$  light, linearly polarized at  $\sim 45^\circ$  to vertical, into the waveguides. Modulation of the signal was achieved by placing a polarizer at the output of the waveguide and applying either a dc or dc+ac voltage across the device electrodes. Figure 2 shows the response of the modulator to an applied dc voltage. The data were taken as follows: a positive 100 V bias (50 kV/cm) was applied to the sample for a few minutes prior to data acquisition (well in excess of the coercive field for the film,  $\sim 15$  kV/cm); then, starting at 0 V, a potential was applied in  $-5$  V ( $-2.5$  kV/cm) increments to  $-90$  V ( $-45$  kV/cm) ( $\square$  data points); the potential was then incrementally increased to  $+90$  V ( $\triangle$  data points); and finally reduced back to zero ( $X$  data points). We could not measure any current flow across the electrode gap with 100 V (50 kV/cm) applied and an ammeter sensitivity of  $10^{-7}$  A. At lower fields there were small changes, over a period of hours, in the polarization of the light emerging from the output of the waveguide, which caused relatively small changes ( $<10\%$ ) in the signal amplitude at the detector. It is not clear whether the changes in signal throughput were caused by domain movement or current flow between the electrodes. Higher fields ( $>35$  kV/cm), however, produced relatively large changes in signal

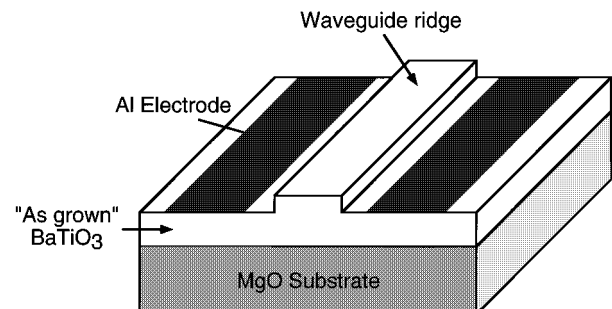


FIG. 1. Schematic representation of the ridge waveguide modulator structure.

<sup>a)</sup>Department of Electrical and Computer Engineering.

<sup>b)</sup>Also with: Department of Materials Science and Engineering.

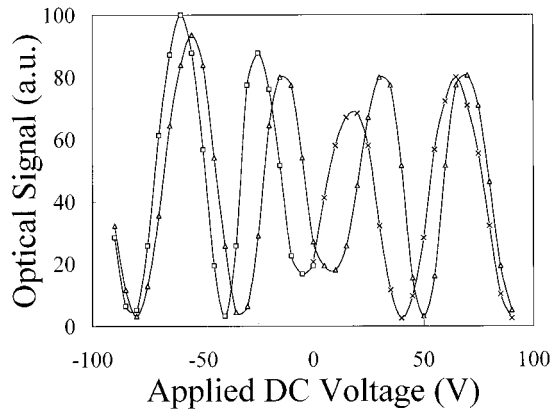


FIG. 2. Amplitude modulation in an “as-grown” thin-film BaTiO<sub>3</sub> channel waveguide vs applied dc voltage. The data were taken as follows: a positive voltage was applied to the electrodes prior to data acquisition; then, starting at 0 V a negative potential was applied in 5 V increments up to -90 V ( $\square$  data points); the potential was then increased from -90 V to +90 V ( $\triangle$  data points); and, finally, reduced from +90 V back to zero ( $\times$  data points).

throughput, possibly caused by current flow and heating in the film.

The frequency ( $\nu$ ) dependence of the modulator response was determined from 0 to 5 MHz by measuring the amplitude modulation of the output light using an InGaAs detector and an oscilloscope (for  $0 < \nu < 500$  Hz), lock-in amplifier (for  $500 \text{ Hz} < \nu < 100$  kHz), and spectrum analyzer (for  $\nu > 100$  kHz). The applied field for the ac measurements consisted of an ac superposed on a 15 kV/cm dc field. Care was taken to ensure that the change in signal throughput was monotonic with applied voltage and that the modulation depth was less than  $\pi/2$  for the lock-in amplifier and spectrum analyzer measurements.

Figure 2 shows the modulation of 1.55  $\mu\text{m}$  light as a function of applied dc voltage for a 2.5  $\mu\text{m}$  wide waveguide with a 20  $\mu\text{m}$  electrode gap and 2.7 mm long electrodes. A hysteresis in the modulator response is seen, since the throughput is dependent on whether the bias is increasing or decreasing. The hysteresis is less evident at higher field strengths. The hysteresis could result from reversible poling by the applied field and/or space-charge formation in the film. Modulation depths in excess of 14 dB were measured. The modulator went from an “on” state with a  $\sim 30$  V bias (15 kV/cm) to an “off” state with a  $\sim 50$  V bias (25 kV/cm). Therefore, a  $\pi$  phase shift is induced between the TE and TM polarization path lengths in the waveguide with a  $20 \pm 2$  V change in applied bias, we call this the half-wave voltage change,  $\Delta v_\pi$ .

The electro-optic response of the film to the applied field is complex, and as yet, not fully understood. Presumably, domain alignment dominates at lower field strengths ( $< 15$  kV/cm). Once the coercive field strength is reached, the film is assumed to have a net polarization with the  $+c$  axis parallel to the field direction. In this initial experiment, we measure the relative change in the wavelength propagation indexes between the TE and TM polarizations,  $\Delta n_{\text{TE}}^{\text{eff}} - \Delta n_{\text{TM}}^{\text{eff}} = \Delta n_{\text{TE-TM}}^{\text{eff}}$ , under an applied field parallel to the TE polarization. Modeling of the channel waveguide structure indicates that a relative index change in the film,  $\Delta n_{\text{TE}} - \Delta n_{\text{TM}} = \Delta n_{\text{TE-TM}}$ , of  $3.25 \times 10^{-4}$  will produce a half-wave phase

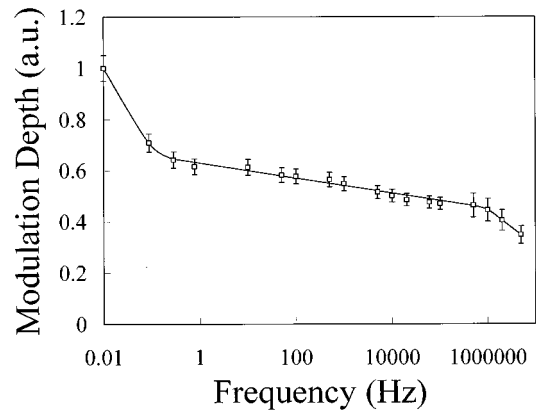


FIG. 3. Modulation depth versus frequency for 1.3  $\mu\text{m}$  light in a 7  $\mu\text{m}$  wide waveguide with 1.6 mm long electrodes, 20  $\mu\text{m}$  electrode gap, 30 V dc bias, and a 22 V peak-to-peak ac bias.

shift between the TE and TM polarizations in the waveguide, this corresponds to a waveguide propagation index change of  $\Delta n_{\text{TE-TM}}^{\text{eff}} \sim 2.87 \times 10^{-4}$  as explained in Ref. 10 [assuming a bulk index value for the film  $n_{\text{film}} = 2.35$  (Ref. 11) and  $n_{\text{substrate}} = 1.7$ ]. The effective electro-optic coefficient of the film is then estimated assuming the change in the electric field  $\Delta E_\pi \sim \Delta V_\pi/d$ , where  $d$  is the electrode spacing. We also assume 100% overlap between the electric field and the film. These assumptions are reasonable since the dielectric constant of the film is much higher than that of the substrate and air. It should be noted that the formation of space charge in the film could strongly reduce the actual field seen by the film, however, these effects are neglected here. The effective electro-optic coefficient is defined to be

$$\Delta r^{\text{eff}} = r_{\text{TE}}^{\text{eff}} - r_{\text{TM}}^{\text{eff}} = \frac{1}{\Delta E_\pi} \left[ \left( \frac{1}{n_{\text{TE}}^\pi} \right)^2 - \left( \frac{1}{n_{\text{TE}}} \right)^2 \right] - \left[ \left( \frac{1}{n_{\text{TM}}^\pi} \right)^2 - \left( \frac{1}{n_{\text{TM}}} \right)^2 \right], \quad (1)$$

where  $n_{\text{TE(TM)}}^\pi$  and  $n_{\text{TE(TM)}}$  are the refractive indices of the TE(TM) polarization before and after the  $\Delta V_\pi$  change in the applied voltage, respectively. Therefore, by Ref. 12,

$$\Delta r^{\text{eff}} \approx \frac{2 \Delta n_{\text{TE-TM}}}{\Delta E_\pi (n_{\text{film}})^3}. \quad (2)$$

This yields an effective dc electro-optic coefficient of  $\Delta r^{\text{eff}} \sim 50 \pm 5$  pm/V for the film. It should be noted that the effective electro-optic coefficient contains the field induced index changes from domain poling, domain-wall movement, and the linear electro-optic effect. Similar results were found for 1.3  $\mu\text{m}$  light.

The BaTiO<sub>3</sub> thin film showed both linear and quadratic electro-optic responses when the modulator was operated with an ac bias superposed on a dc bias. At  $\sim 0$  V dc bias, the film showed a relatively weak quadratic electro-optic response. As the dc bias was increased, the electro-optic response became much stronger and linear, since higher-order harmonic components in the modulated signal were not observed.

Modulation depth as a function of frequency is shown in Fig. 3 (for 1.3  $\mu\text{m}$  light in a 7  $\mu\text{m}$  wide waveguide with 1.6 mm long electrodes, 20  $\mu\text{m}$  electrode gap, 30 V (15 kV/cm)

dc bias, and a 22 V (11 kV/cm) peak-to-peak ac bias). The modulation depth decreases to  $\sim 60\%$  of the dc value when operated at  $\sim 1$  Hz; at 20 kHz the modulation depth is  $\sim 50\%$  of the dc value, and from 20 kHz to 5 MHz, the modulation depth shows a slower roll-off to  $\sim 37\%$  of the dc value. Modulation of the signal was observed at frequencies in excess of 5 MHz. The data indicate that several mechanisms contribute to the measured electro-optic effect, evidenced by the changing slope in Fig. 3. The large drop in  $r_{\text{eff}}$  from dc to 1 Hz operation is presumably caused by the slow response of the domain reorientation in the film. The more modest drop from 1 Hz  $\gg \nu > 20$  kHz, and 20 kHz  $\gg \nu > 5$  MHz is most likely indicative of more subtle domain-wall movement. We did not see any fatigue effects. There was also no degradation in modulator performance from repeatedly reversing the applied bias or after months of testing. However, we did see a degradation in modulator performance that seemed to be related to high humidity, which was eliminated by baking the structure at  $\sim 120$  °C. Higher frequency measurements are needed to determine the relative contribution to the modulation from the linear electro-optic effect. We are in the process of fabricating optimized structures to measure the electro-optic response at frequencies in excess of 5 MHz.

The measured properties of the thin-film BaTiO<sub>3</sub> electro-optic modulator can be used to calculate the performance of a more optimized device. Previous measurements of waveguide output spot size versus waveguide width indicate that a 5  $\mu\text{m}$  electrode spacing could easily be used for a 2.5  $\mu\text{m}$  wide waveguide.<sup>5</sup> Therefore, a 2.5  $\mu\text{m}$  wide waveguide modulator with 1 cm long electrodes and a 5  $\mu\text{m}$  electrode gap should have a dc half-wave voltage of 1.35 V with a bias of 2 V in an "as-grown" film. This corresponds to a VL product of 1.35 V cm, we estimate the VL product at 5 MHz to be  $\sim 4$  V cm.

In conclusion, a simple channel waveguide modulator has been fabricated in epitaxial BaTiO<sub>3</sub> on MgO. Electro-optic modulation of 1.3 and 1.55  $\mu\text{m}$  light was demonstrated. Films had an effective electro-optic coefficient,  $\Delta r_{\text{eff}}$ , of  $\sim 50 \pm 5$  pm/V for applied dc voltages and  $\sim 18 \pm 2$  pm/V at 5 MHz. Epitaxial thin-film BaTiO<sub>3</sub>, therefore, offers the poten-

tial for low-voltage highly confining guided wave electro-optic modulator structures.

This work is supported by the AFOSR/ARPA under Award No. F49620-96-1-0262 and the MRSEC program of the National Science Foundation at the Materials Research Center (MRC) of Northwestern University under Award No. DMR-9632472. This work made extensive use of the MRC crystal growth and materials processing facility.

<sup>1</sup>D. K. Fork, F. Armani-Leplingard, and J. J. Kingston, Mater. Res. Soc. Symp. Proc. **361**, 155 (1995).

<sup>2</sup>G. N. van den Hoven, R. J. I. M. Koper, A. Polman, C. van Dam, J. W. M. van Uffelen, and M. K. Smit, Appl. Phys. Lett. **68**, 1886 (1996).

<sup>3</sup>D. K. Fork, F. Armani-Leplingard, J. J. Kingston, and G. B. Anderson, Mater. Res. Soc. Symp. Proc. **392**, 189 (1996).

<sup>4</sup>F. J. Walker, R. A. McKee, Huan-wun Yen, and D. E. Zelmon, Appl. Phys. Lett. **65**, 1495 (1994).

<sup>5</sup>D. M. Gill, B. A. Block, C. W. Conrad, B. W. Wessels, and S. T. Ho, Appl. Phys. Lett. **69**, 2968 (1996).

<sup>6</sup>M. Zgonik, P. Bernasconi, M. Duelli, R. Schlessler, P. Gunter, M. H. Garret, D. Rytz, Y. Zhu, and X. Wu, Phys. Rev. B **50**, 5941 (1994).

<sup>7</sup>L. A. Wills, W. A. Feil, B. W. Wessels, L. M. Tonge, and T. J. Marks, J. Cryst. Growth **107**, 712 (1991).

<sup>8</sup>The preferred orientation cannot be uniquely determined by x-ray diffraction due to residual strain in the film. This strain modifies the lattice constant to be less than the bulk *c*-axis lattice constant and greater than the *a*-axis constant.

<sup>9</sup>B. A. Block, B. W. Wessels, M. J. Nystrom, D. M. Gill, and S. T. Ho, Mater. Res. Soc. Symp. Proc. (to be published).

<sup>10</sup> $n_{\text{TE(TM)}}^{\text{eff}}$  is the effective propagation index of the TE(TM) polarization in the composite of substrate, film, and air, which comprise the volume of the propagation mode.  $n_{\text{TE(TM)}}^{\text{eff}}$  is related to  $n_{\text{TE(TM)}}$ , the actual TE(TM) index of the film, through the guiding angle of the waveguide structure,  $\theta$ , such that  $n_{\text{TE(TM)}}^{\text{eff}} = n_{\text{TE(TM)}} \cos \theta_{\text{TE(TM)}}$ . We note that  $\Delta n_{\text{TE(TM)}}^{\text{eff}} = n_{\text{TE(TM)}}^{\text{eff}}(\phi_{\pi}) - n_{\text{TE(TM)}}^{\text{eff}}(\phi_0)$  where  $n_{\text{TE(TM)}}^{\text{eff}}(\phi_0)$  and  $n_{\text{TE(TM)}}^{\text{eff}}(\phi_{\pi})$  are the TE(TM) waveguide propagation indexes before and after the half-wave voltage change,  $\Delta V_{\pi}$ , respectively.  $\Delta n_{\text{TE-TM}}^{\text{eff}} = \Delta n_{\text{TE}}^{\text{eff}} - \Delta n_{\text{TM}}^{\text{eff}}$ . We measure  $\Delta n_{\text{TE-TM}}^{\text{eff}}$  and calculate  $\Delta n_{\text{TE-TM}}$  noting that  $\theta_{\text{TE}} \approx \theta_{\text{TM}} = \theta$ . Therefore,  $\Delta n_{\text{TE-TM}}^{\text{eff}} = \Delta n_{\text{TE}}(\cos \theta_{\text{TE}}) - \Delta n_{\text{TM}}(\cos \theta_{\text{TM}}) \approx (\Delta n_{\text{TE}} - \Delta n_{\text{TM}})(\cos \theta) = \Delta n_{\text{TE-TM}}(\cos \theta)$ .

<sup>11</sup>A. R. Johnson, J. Appl. Phys. **42**, 398 (1971).

<sup>12</sup>[Equation (1)] =  $\{[(n_{\text{TE}} + n_{\text{TE}}^{\pi})(n_{\text{TE}} - n_{\text{TE}}^{\pi}) / (n_{\text{TE}}^2 n_{\text{TE}}^{\pi 2})] - [(n_{\text{TM}} + n_{\text{TM}}^{\pi})(n_{\text{TM}} - n_{\text{TM}}^{\pi}) / (n_{\text{TM}}^2 n_{\text{TM}}^{\pi 2})]\} / \Delta E_{\pi} \approx [(2n_{\text{TE}} \Delta n_{\text{TE}} / n_{\text{TE}}^4) - (2n_{\text{TM}} \Delta n_{\text{TM}} / n_{\text{TM}}^4)] / \Delta E_{\pi}$ ,  $n_{\text{TE}} \approx n_{\text{TM}} = n_{\text{film}}$ . Therefore,  $\Delta r_{\text{eff}}^{\text{eff}} \approx 2(\Delta n_{\text{TE}} - \Delta n_{\text{TM}}) / \Delta E_{\pi} (n_{\text{film}})^3 = 2\Delta n_{\text{TE-TM}} / \Delta E_{\pi} (n_{\text{film}})^3$ .